processes

Article

Numerical Investigation of the Heat and Mass Transfer during the In Situ Pyrolysis Process of Oil-Rich Coal

Fu Yang [1,2,†], Xiangqiang Cheng [2,†], Mingjie Li [2,*], Jinjia Wei [2], Zhonghui Duan [1] and Li Ma [1,3]

1 Shaanxi Provincial Coal Geology Group Co., Ltd., Key Laboratory of Coal Resources Exploration and Comprehensive Utilization, Ministry of Natural Resources, Xi'an 710026, China
2 School of Chemical Engineering and Technology, Xi'an Jiaotong University, Xi'an 710049, China
3 School of Electrical Engineering, Xi'an Jiaotong University, Xi'an 710049, China
* Correspondence: mjli2018@mail.xjtu.edu.cn
† These authors contributed equally to this work.

Abstract: A multi-physics numerical method coupling fluid flow, heat transfer, and a chemical reaction was used to determine the temperature distribution and the conversion rate of a coal seam during underground pyrolysis. The coal seam was fractured to enhance the heat and mass transfer. The influences of the pyrolysis pressure on the heat transfer, oil and gas production, and pyrolysis time were also analyzed. When the injection gauge pressure was increased to 14 MPa, the conversion rate on the 120th day was 98.8% and the promotion was not obvious any more at further higher pressures for the model without a fracture. For the model with a fracture, the pyrolysis was completed in only 90 days at the much lower pressure of 4 MPa, which is beneficial for both reducing the heating period and enabling the rapid harvesting of oil. Then, the fractured zone was designed and optimized by investigating different radii of the fractured zone at both the inlet and the outlet of the domain. The dead zones around the two corners at the right side of the computational domain near the outlet well were reduced effectively with an increase in the diameter of the fractured region. The heat and mass transfer were enhanced with a larger area of the fractured region at the outlet well for the reason that the flowing dead zones experienced a longer effective heating time.

Keywords: oil-rich coal; in situ pyrolysis; multi-physics; simulation

Citation: Yang, F.; Cheng, X.; Li, M.; Wei, J.; Duan, Z.; Ma, L. Numerical Investigation of the Heat and Mass Transfer during the In Situ Pyrolysis Process of Oil-Rich Coal. *Processes* **2023**, *11*, 3226. https://doi.org/10.3390/pr11113226

Academic Editors: Ireneusz Zbicinski, Lei Qin and Ruiyue Yang

Received: 14 October 2023
Revised: 7 November 2023
Accepted: 9 November 2023
Published: 14 November 2023

1. Introduction

Oil-rich coal is the coal with a dry oil base yield of 7–12%. It has a hydrogen-rich structure, which can generate a good deal of oil and gas through pyrolysis. It is regarded as a special coal resource that integrates oil and coal properties [1]. In Shaanxi, more than 170 billion tons of coal have been identified, and oil-rich coal accounted for more than 85 percent. Oil-rich coal is mainly distributed in the Jurassic coal field, the Triassic coal field, and the Carboniferous Permian coal field of northern Shaanxi and the Huang long Jurassic coal field with resources of up to more than 150 billion tons, and a large number of tars can be extracted, especially in the Yulin area [2]. The in situ pyrolysis of oil-rich coal is an emerging coal-utilization technology in recent years that involves heating and pyrolyzing coal reservoirs underground through a heat carrier without mining. Similar to the in situ pyrolysis or upgrading of oil shale [3–5], the coal needs to be heated to the pyrolysis temperature using a heat carrier with a high temperature and pressure. Meanwhile, the oil and gas products diffuse through the artificial cracks and pores in the coal reservoir and are eventually exported to the ground through wells for subsequent separation and deep processing. The in situ pyrolysis of oil-rich coal is economical, sustainable, and environmentally friendly, with a lower mining cost compared with ground pyrolysis, and thus, it has received more and more attention recently. The process of in situ pyrolysis is shown in Figure 1.

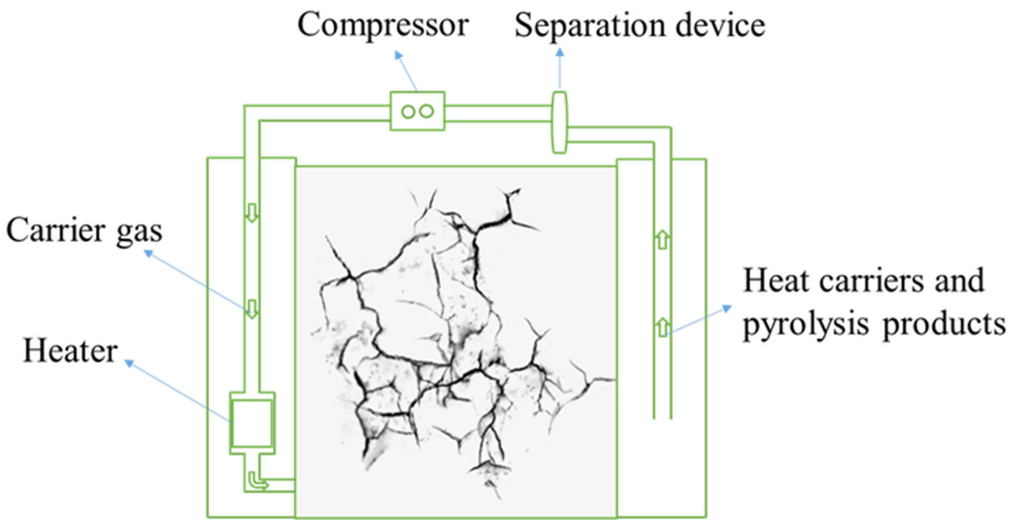

Figure 1. Schematic diagram of oil-rich coal in situ pyrolysis.

During in situ pyrolysis or upgrading, the chemical and physical characteristics of the coal as well as the heat carrier greatly influence the reservoir temperature and the chemical reaction rate, which, in turn, have an effect on the total heat consumption and efficiency of the process. Thus, it is crucial to determine the temperature distribution of the coal reservoir, the pressure of the heat carrier injection, the properties of the coal seam, and so on to obtain an optimal oil and gas production and heating efficiency.

To improve the heating efficiency, researchers have chosen various heat patterns to optimize the pyrolysis process. For example, Song et al. [6] proposed a scheme of multiple wells instead of vertical wells to simulate the conversion process of oil shale, and the heating efficiency can be improved by this method. Using horizontal wells with nine stages of hydraulic fracturing as a model, Mukhina et al. [7] found that the method of hot water steam injection had the highest oil recovery. Maes et al. [8] simulated a simplified heater pattern and found that the dimensionless Damköhler number plays an important role in controlling the reaction time and improving the process efficiency. Lee et al. [9] simulated the pyrolysis of kerogen and hydrocarbon production with production wells at different locations in the reservoir. The effects of the vertical heater temperature and the hydraulic fracture spacing were analyzed.

In addition to the heating mode, the choice of heat carrier is also crucial to the pyrolysis effect. For example, Pei et al. [4] simulated the nitrogen-injection-assisted in situ conversion process using a reaction model of kerogen pyrolysis at a high temperature. The oil production and the energy efficiency were increased by a nitrogen injection. Then, they proposed assisting the in situ upgrading process with an air injection [3,10] and compared it with a N_2 injection for field applications. Wang et al. [11] heated oil shale by steam, and, combined with the flow field distribution in a numerical simulation, it explained the trend in the oil shale permeability change and cracking characteristics under a high temperature. Lee et al. [12] took steam or high-temperature water injections into well systems to obtain the temperature distribution of the reservoir and fluid production, given the positions of the horizontal wells.

Some researchers focus on the reservoir and its physicochemical characteristics. Based on a two-dimensional model. Gao et al. [13] simulated the growth of cavitation using a model of porosity change during underground coal gasification. The simulation results are similar as the experimental results. Panahi et al. [14] investigated the impact of heating rate using ground experiments and 3D X-ray microtomographic images. It has been found that fracturing could influence the heating rate and the final temperature, which further affects the fluid expulsion. Jiang et al. [15] developed a 3D model to account for the pore variations, weight loss of coal and solid concentrations during underground coal gasification and combustion. Wang et al. [16] determined the thermal, hydraulic, mechanical and other properties of oil shale. They also simulated the distribution of pressure, temperature, permeability and other parameters during in situ gas extraction. Yuan et al. [17] simulated the effects of geomechanics and the thermal recovery coupling fluid flow. They investigated the impact of different parameters (temperature, bottom hole pressure and Langmuir volume) on heat recovery efficiency. Hu et al. [18] conducted an investigation into the stress distribution, which revealed that the heterogeneous expansion of minerals under electromagnetic heating leads to greater tension, as indicated by numerical simulations.

The above research mainly focuses on the pyrolysis of oil shale, with few studies addressing the pyrolysis of oil-rich coal, particularly involving chemical reactions. Relevant research on underground coal gasification can also provide reference. Alfarge et al. [19] also utilized the commercial CMG-GEM simulator to study the impact of CO_2 injection into shale-oil reservoirs with five hydraulic fractures, considering the molecular-diffusion of CO_2. The numerical model indicates that the molecular diffusion of CO_2 is crucial. In addition, underground coal gasification can also provide valuable insights. Gür et al. [20] utilized Fluent to simulate the composition and temperature variations of syngas. Xi et al. [21] conducted a numerical simulation of multi-physics coupling using COMSOL Multiphysics for underground coal gasification. By taking temperature as the coupling variable and the gasification reaction heat of coal seam as the source term, the temperature field was solved. Only the diffusion of CO_2, H_2, CH_4 and CO of gases was considered in the calculation process, and the consumption of fixed coal seam and the total product cannot be effectively predicted.

From the brief literature review above, we can see that temperature and production distribution (oil components and gas components) are crucial during pyrolysis. However, the thermal conductivity of the coal is rather low, at 0.3 $W \cdot m^{-1} \cdot K^{-1}$, making it difficult to heat. In addition, the conversion rate of the coal reservoir cannot be accurately predicted due to the multi-physics of in situ pyrolysis of oil-rich coal and the coupled problem between chemical reaction and temperature transportation; hence, the oil and gas production could not be precisely forecasted, either. In this paper, a multi-physics numerical method is used to determine the temperature distribution and the conversion rate of the reservoir in the porous fracture region. The coal reservoir is fractured to enhance the heat and mass transfer. The fractured zone is designed and optimized by investigating different radii of the fractured zone both at the inlet and outlet of the domain. The effects of the pyrolysis pressure and pyrolysis time on heat transfer, as well as production, are also analyzed. It can offer effective guidance and support for the pilot project involving the in situ pyrolysis of oil-rich coal, leading to further energy savings and efficiency improvements.

2. Model Description

2.1. Computational Domain and Boundary Conditions

The actual production process of the in situ pyrolysis of oil-rich coal is shown in Figure 1. Nitrogen gas is heated and injected into the fractured zone to heat the coal seam. The coal seam starts pyrolysis when the temperature exceeds 573 K, and oil and volatile gas are then generated. The products flow out with the high-temperature nitrogen through the production well. Oil and volatile gas are subsequently collected and separated and purified to produce high value organic matter. The permeability of the coal seam is increased by fracturing the middle area of the coal seam around the inlet or outlet wells whether through hydraulic fracturing or shock wave fracturing so as to enhance the mass and heat transfer. The computing domain is shown in Figure 2. The side length of the square geometric model is 10 m. High-temperature nitrogen flows into the computing domain from the entrance with a length of 0.1 m. The fluid flows out from the outlet which is a length of 0.1 m on the right side. The surrounding walls are set as symmetry boundaries. The dashed line in the figure indicates different areas of the fractured zone with higher permeability attributed to hydrofracturing or shock wave fracturing, which will be discussed particularly in Sections 3.2 and 3.3. The areas with different colors represent the size area of the fractured zone.

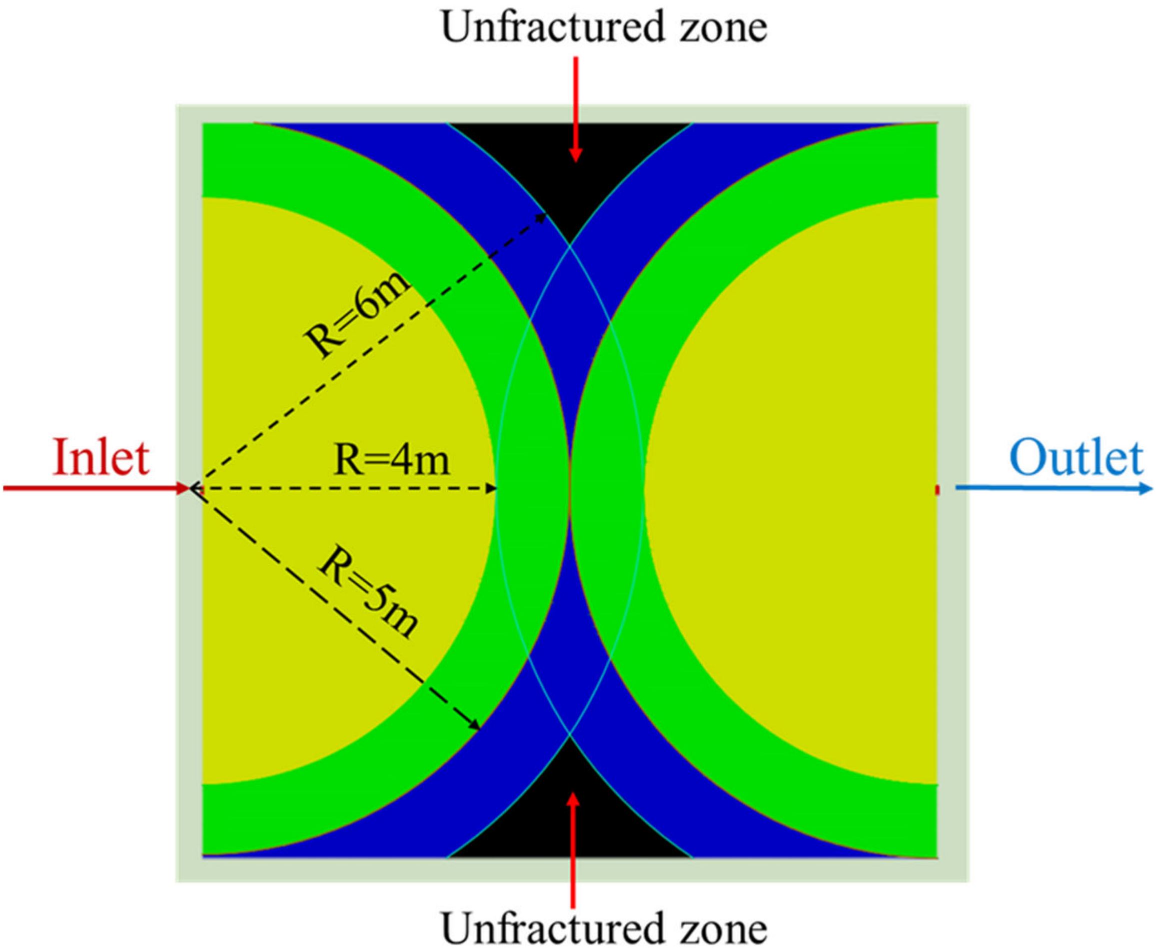

Figure 2. Computational domain and boundary conditions.

To reduce the computation cost of simulation, the following assumptions are conducted:

(1) The actual geometric model is simplified into a two-dimensional computational region;
(2) Radiative heat transfer is not considered in the process of in situ pyrolysis underground;
(3) Many fissures and cracks exist in the center, simplifying the computational domain into a porous media region;
(4) The pyrolysis reaction occurs at which the temperature is higher than 573 K according to pyrolysis experiments, and thus, the oil and volatile gases in the products are assumed to be in the gaseous state.

2.2. Chemical Reaction Model

Many scholars have studied the related products and reaction kinetics of coal pyrolysis. Hu et al. investigated the typical products of coal pyrolysis by mass spectrometry and found that the oil products mainly include four categories: alkenes, aromatic hydrocarbons, monophenols and diphenols [22,23]. The pyrolysis reaction formula of oil-rich coal is obtained by ground experiments to simulate the underground pyrolysis of oil-rich coal. It is found that almost no volatile gas is generated and only involves the production of water (when T < 573 K). The volatile gas and the oil are generated (when T > 573 K). The reaction equation can be expressed as follows:

From 293 to 573 K:

$$Coal \xrightarrow{293\ \mathrm{K}-573\ \mathrm{K}} Coal' + 56.93H_2O \tag{1}$$

And from 573 to 873 K:

$$Coal' \overset{573\ \text{K}-873\ \text{K}}{\rightarrow} Char + Oil + Gas + 15.23H_2O \tag{2}$$

where the oil in the product consists of the following species:

$$Oil = 0.45\text{C}_{10}H_8 + 0.28\text{C}_{12}H_8O + 0.35\text{C}_{13}H_{10} + 1.65\text{C}_{14}H_{10} + 1.40\text{C}_{16}H_{10} \tag{3}$$

$$Gas = 11.67CO + 37.58CH_4 + 31.00CO_2 + 19.75H_2 \tag{4}$$

Since the phenomenon of volume contraction during the formation of char is not obvious and the internal diffusion of gases in the solid controls the speed of the reaction, the internal diffusion velocity control model with constant solid volume is used to describe the reaction (when T > 573 K).

The activation energy related to temperature could be solved by the reaction kinetics model function. Some scholars obtained these parameters by the common KAS method [24,25]. In order to simplify the analysis, most scholars choose the single scan rate method. The Coats–Redfern integral method we used which is a dynamic analysis method based on the experimental results at a certain programmed temperature rate [26,27].

The non-isothermal thermal decomposition reaction of solids is expressed by the following equation:

$$\frac{d\alpha}{dt} = kf(\alpha) \tag{5}$$

where $f(\alpha)$ is mechanism function of the pyrolysis reaction, and the reaction conversion rate α is calculated by:

$$\alpha = \frac{m_0 - m}{m_0 - m_\infty} \tag{6}$$

where m_0 is the initial value of mass of the reactant, m is the mass of the reactant at a given moment, and m_∞ is the mass of the reactant after the complete reaction. k is the rate constant evaluated by the Arrhenius equation. Substituting it into Equation (5), we can obtain the following:

$$\frac{d\alpha}{dt} = A \times exp\left(\frac{-E}{RT}\right) f(\alpha) \tag{7}$$

where A is the pre-exponential factor of the reaction, R is the ideal gas constant and E is the activation energy of the reaction. These parameters of pyrolysis are obtained through experiments whose values are shown in Table 1.

Table 1. Kinetic parameters of pyrolysis.

Temperature (K)	E (kJ·mol^{-1})	A (min^{-1})	R^2
573–873	72.35	414.6	0.9902

2.3. Mass and Heat Transfer Model

For the pyrolysis model of oil-rich coal, the products exist in the form of gas. Nitrogen, which serves as the heat carrier injected through heating well, does not participate in the reaction. Thus, the mass balance equation of the gas is as follows:

$$\frac{\partial(\rho_g \varphi_N \varepsilon)}{\partial t} + \nabla\left[\rho_g \varphi_N \mathbf{u} + D\rho_g \nabla\varphi_N\right] = \dot{m_N} \tag{8}$$

where φ_N is molar fraction of the gas component including volatile gas, oil, and water, ε is the porosity of the porous medium, D is the diffusion coefficient, and $\dot{m_N}$ represents the mass source term. The source term $\dot{m_{N_2}}$ is equal to zero, as N_2 does not participate in the pyrolysis reaction. The corresponding mass source term of the remaining gas components are represented by Equation (9).

$$\dot{m_N} = M_N \cdot r \tag{9}$$

where M_N is the molar mass of the substance, and r is the reaction rate which is related to the conversion rate. $\mathbf{u}$ is the apparent gas velocity of the gas mixture. It is determined by Darcy's law, as shown in Equation (10). ϑ represents the permeability of the porous medium, μ_g is the power viscosity of the gas mixture, and ∇p represents the pressure drop when fluids flow through the porous medium.

$$\mathbf{u} = \frac{\vartheta}{\mu_g} \nabla p \tag{10}$$

The energy balance equation of the pyrolysis reaction is given by

$$\frac{\partial}{\partial t}\left(\left(\rho c_p\right)_{\text{eff}} T\right) + \left(\rho c_p\right)_{\text{g}} \mathbf{u} \nabla T + \nabla(\lambda_{\text{eff}} \nabla T) = \dot{Q} \tag{11}$$

$\dot{Q}$ is the energy source which represents the heat absorption of the pyrolysis reaction as shown in Equation (12)

$$\dot{Q} = -\Delta H_R \cdot r \tag{12}$$

c_p is the specific heat capacity of the substance, while $\left(\rho c_p\right)_{\text{eff}}$ represents the equivalent heat capacity and density of the gas-solid two-phase. λ_{eff} is the equivalent thermal conductivity, which is calculated as shown in Equations (13) and (14). The corresponding parameter values are shown in Table 2.

$$\left(\rho c_p\right)_{\text{eff}} = \varepsilon\left(\rho c_p\right)_{\text{g}} + (1-\varepsilon)\left(\rho c_p\right)_{\text{s}} \tag{13}$$

$$\lambda_{\text{eff}} = \varepsilon \lambda_{\text{g}} + (1-\varepsilon)\lambda_{\text{s}} \tag{14}$$

Table 2. Parameter of the simulation and initial conditions.

Parameters/Unit	Value
$\varepsilon/100\%$	0.2
ϑ/mD	1
$\rho_s/\text{kg}\cdot\text{m}^{-3}$	1300
$c_{p,s}/\text{J}\cdot\text{kg}^{-1}\cdot\text{K}^{-1}$	1000
$\lambda_{\text{eff}}/\text{W}\cdot\text{m}^{-1}\cdot\text{K}^{-1}$	0.239
$M_{Coal}/\text{kg}\cdot\text{mol}^{-1}$	11.67
$M_{Char}/\text{kg}\cdot\text{mol}^{-1}$	7.3
Initial temperature/K	293
Initial pressure/Pa	0

2.4. Grid Independence Verifications

In order to ensure the quality of the grid and improve the efficiency of the generating grid, the structured grid is used, and partial encryption is applied near the boundaries. Different numbers of grids (600, 900, 1656, and 3000) are selected to verify the grid independence. At the same time, the temperature at the center of the domain is detected, and the results are shown in Figure 3. According to the results of the 3rd day, as the number of grids reaches 1656, the maximum difference with that of the grid number of 3000 is only 0.03%. Therefore, the model with the grid number of 1656 is selected for subsequent simulations.

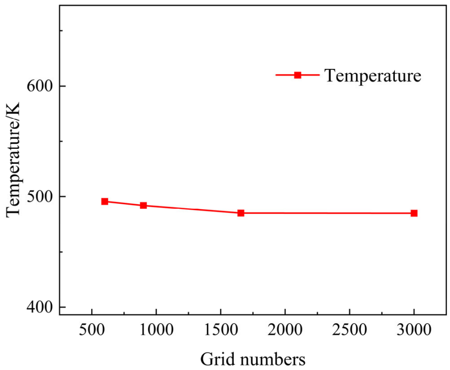

Figure 3. Grid independence verifications.

3. Results and Discussion

3.1. Model Validation

To validate the accuracy of the numerical model of the pyrolysis of oil-rich coal, a pyrolysis experiment of oil-rich coal is conducted in a laboratory at the pressure of 2 MPa with a programmed temperature increase from 293 to 873 K at the rate of 10 K·min^{-1} followed by the constant temperature of 873 K lasing for 30 min. Nitrogen is used as a carrier gas, and the pressure is maintained at 2 MPa. The coal sample is processed into a cylindrical shape. The diameter of the coal sample is 30 mm and the height is 50 mm. The reaction conversion rate α is calculated by Equation (6). The same working conditions and geometric dimensions are adopted in the numerical simulation. The computational domain and the boundary conditions are shown in Figure 4a. The porosity is 0.2. The permeability is 0.1 md in this simulation. The initial temperature and pressure are 293 K and 0 Pa. Numerical and experimental results of the reaction conversion rate of oil-rich coal are shown in Figure 4b. The maximum deviation is less than 5%, and the overall trend of the experimental results is the same with the simulation results. It indicates that the settings of the simulation method and condition are reasonable, and the accuracy of the simulation model is reliable.

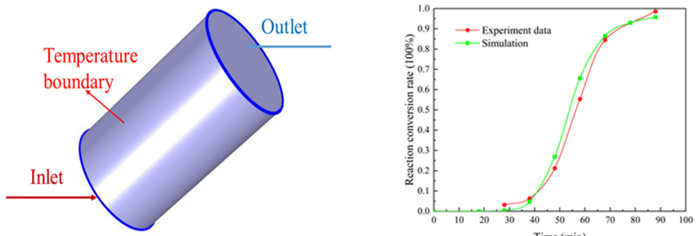

(**a**) (**b**)

Figure 4. The simulation results were compared with the experimental results. (**a**) Computational domain and the boundary conditions; (**b**) Comparison of simulation and experiment results.

3.2. Performance Analysis for In Situ Pyrolysis of Oil-Rich Coal with and without Fracturing inside the Coal Seam

The permeability of the original coal seam underground is rather small generally, and the flow resistance of the heat carrier is huge. Thus, coal seam fracturing is necessary to enhance the heat and mass transfer. The hydrofracturing or shock wave fracturing can be conducted from the injection and the production well to promote the permeability. In this section, the pyrolysis of oil-rich coal underground with and without fracturing inside the coal seam is investigated and compared. For the case without fracturing, the permeability is uniform in the domain and is set as 100 md. For the case with fracturing, hydrofracturing or shock wave fracturing is conducted from the injection and the production wells. The fractured zone is assumed to be circular centered on the inlet and outlet of the nitrogen, as shown in Figure 5. The diameter of the fractured zone is 10 m. The permeability of the fractured zone is set as 1000 md, and the unfractured is 100 md in the simulation. The initial temperature of the coal seam is set to 293 K, and the four boundaries are set as symmetry. The temperature of the inlet nitrogen is 873 K. On account of the low permeability of the unfractured coal, the inlet pressure needs to be high and is set as 20 MPa in this case. The temperature and oil distribution for the cases without fracturing inside the coal seam are shown in Figure 6a,b. From the figure, we can see that it takes 40 days for the hot nitrogen to spread and diffuse to the outlet. During this period, the reaction conversion rate increases linearly with time. Then, the high-temperature region starts to spread from the center zone of the coal to the corners near the outlet. Due to the effect of the fluid dead zone, the slope of the conversion rate decreases, which indicates that the average reaction rate of the pyrolysis also decreases. The temperature increase rate is far too slow; thus, the pyrolysis reaction rate is low, which is displayed in the distribution of production oil in Figure 6b. This leads to high cost of hot fluid injection and heating.

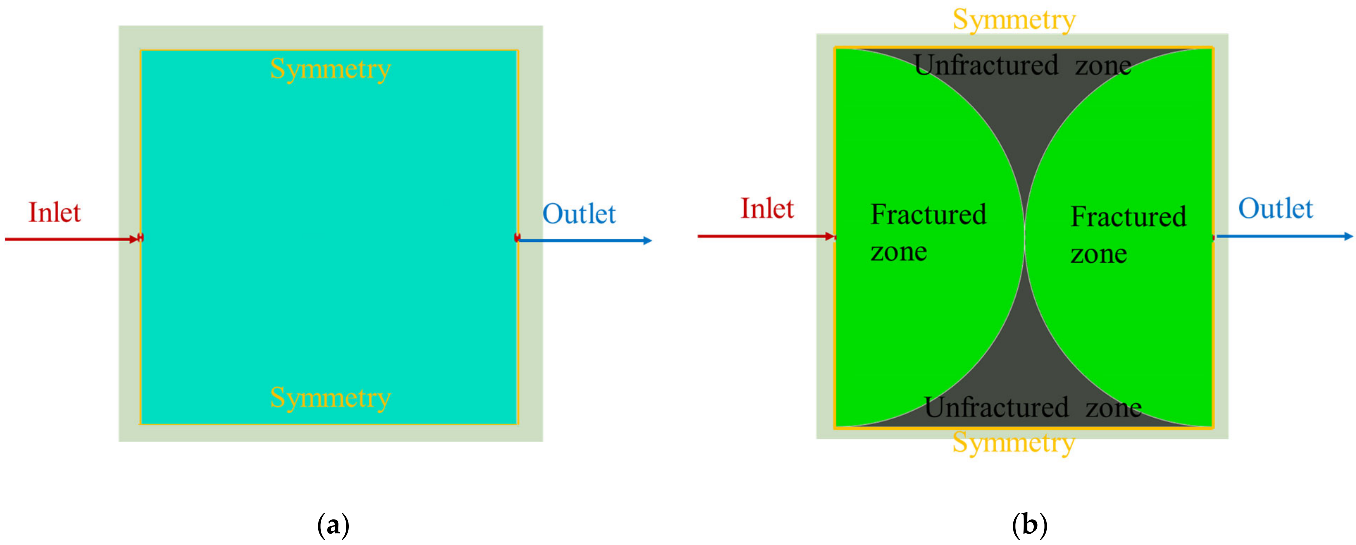

Figure 5. Computational domain and the boundary conditions of the two models without and with fracture. (**a**) Without fracture; (**b**) with fracture.

Then, the effect of injection gauge pressure (ranging from 2–20 MPa) on the pyrolysis performance of the coal reservoir is investigated, and the reaction conversion rate at different inlet pressure (without fracture) is given in Figure 6c. It can be seen that the conversion rate at lower pressure within the same heating period is also small. For example, on the 120th day, the conversion rate is only 25% when the pressure is 2 MPa. With the increase in the injection gauge pressure, the conversion rate increases obviously, and the pyrolysis of oil-rich coal is greatly promoted. The conversion rate reaches 95% at 12 MPa, which means the chemical reaction inside the computational domain is almost completed other than the dead corners of the zone. And the inflection points of the curves with higher pressure appear after the high-temperature region reaches the outlet and starts to spread from the central region to the outer region, as illustrated in Figure 6c. The total reaction time when the pyrolysis is completed also decreases obviously. When the injection gauge pressure is further increased to 14 MPa, the conversion rate on the 120th day is 98.8%, and the promotion is not obvious anymore. Thus, it can be illustrated that the Darcy velocity inside the pores in the coal seam increases linearly with the increase in inlet pressure. But the heat transfer rate from the carrier to the coal seam is not increased as obviously with the increase in Darcy velocity, since the local convection and conduction heat transfer rate and furthermore the chemical reaction rate of the coal seam do not increase linearly. Thus, the inlet pressure no higher than 14 MPa is recommended to enhance the heat and mass transfer during the process of pyrolysis of the oil-rich coal from the aspect of energy saving.

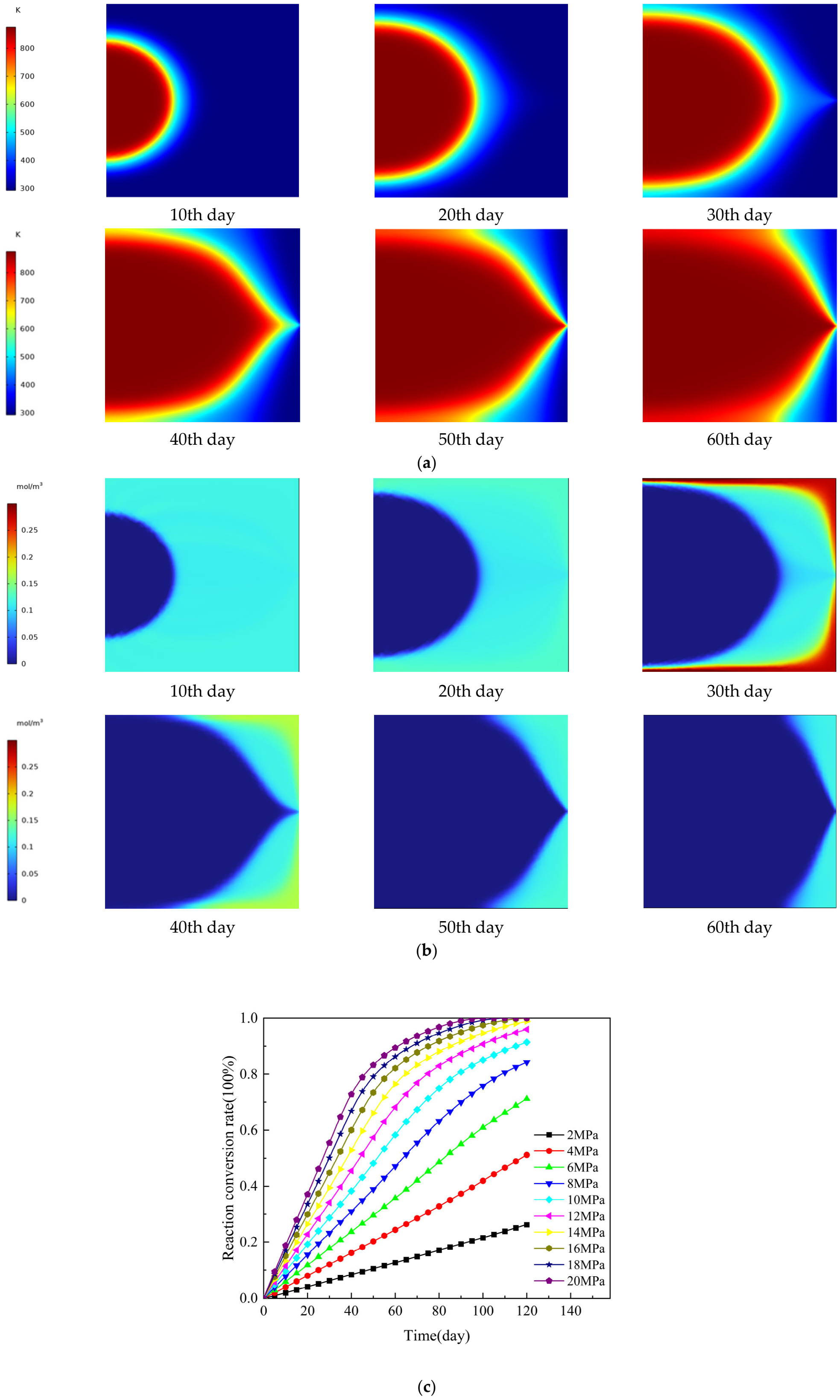

Figure 6. Temperature and oil concentration distribution at pressure inlet of 20 MPa and reaction conversion rate at different inlet pressure (without fracture). (**a**) Temperature distribution; (**b**) distributions of oil concentration; (**c**) reaction conversion rate at different inlet pressure.

Then, the hydrofracturing or shock wave fracturing is conducted, and a computational domain with inhomogeneous permeability as displayed in Figure 5b is employed in the simulation. The temperature and oil concentration distribution at the inlet pressure of 20 MPa are shown in Figure 7a,b. From the figure, we can see that the hot fluid reaches the outlet in only 3 days, which leads to a rapid pyrolysis reaction at the initial stage of the curve. And then the reaction rate slows down due to the spreading from the central region to the corners. But the total pyrolysis time is greatly reduced, and fracturing near the inlet and outlet inside the coal seam could effectively enhance the heat transfer and thus enhance the chemical reaction as well as the mass transfer during the pyrolysis of the oil-rich coal underground. From the reaction conversion rate at different inlet pressures with fracture, as shown in Figure 7c, we can see that the pyrolysis can be completed in only 90 days at a much lower pressure of 4 MPa, which is beneficial for both reducing the heating period and the rapid harvesting of oil production.

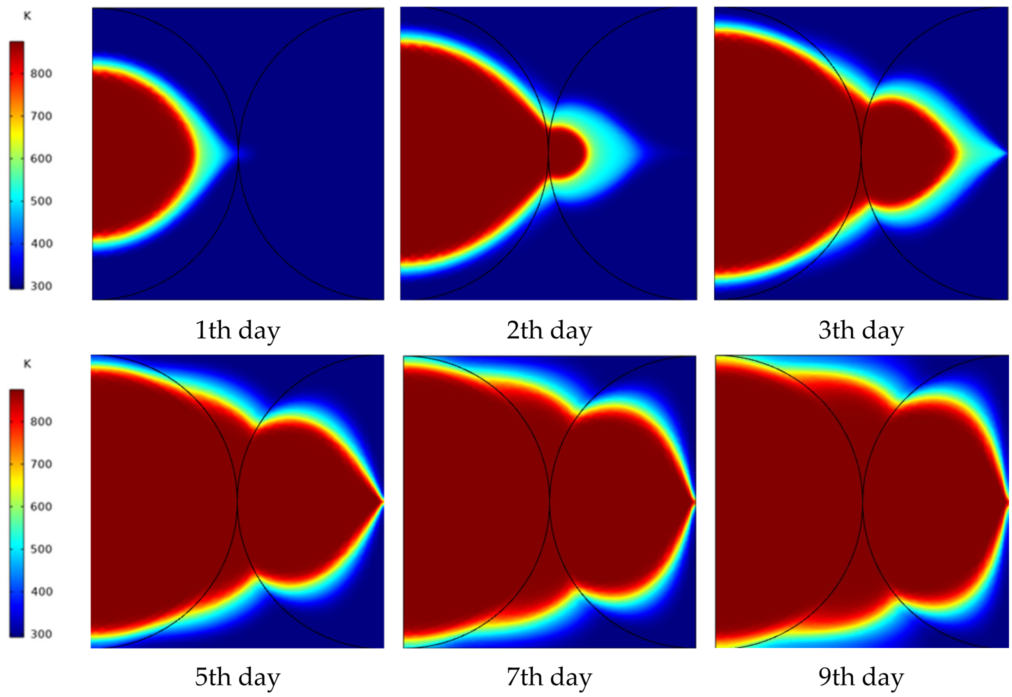

(**a**)

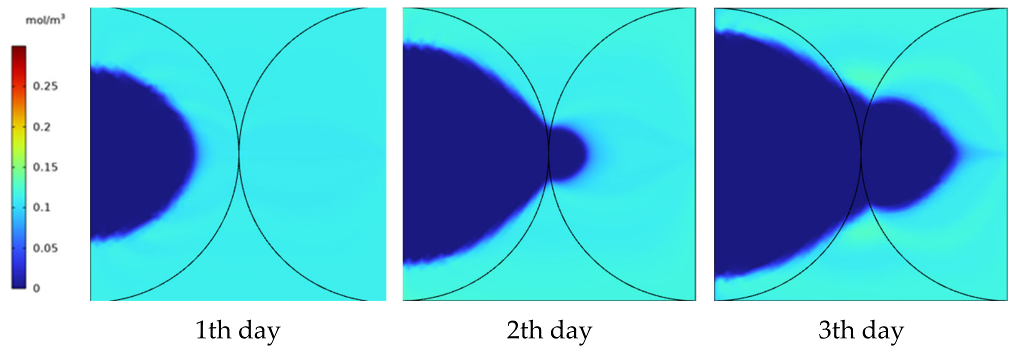

Figure 7. *Cont.*

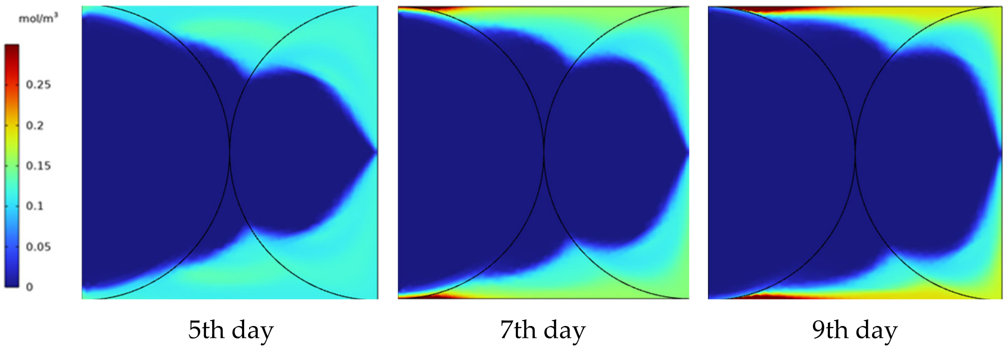

(**b**)

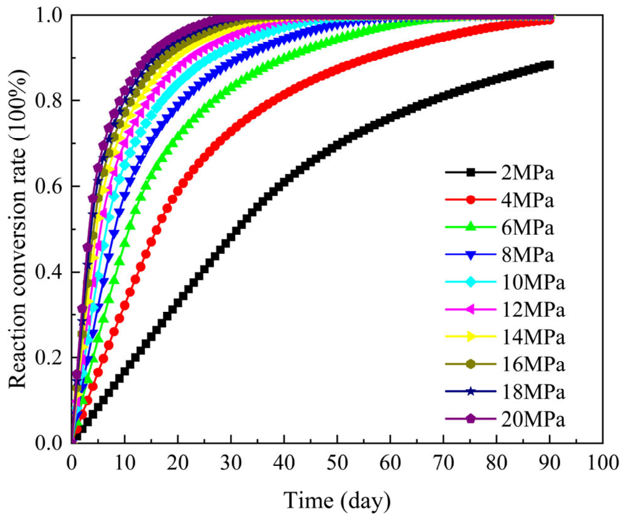

(**c**)

Figure 7. Temperature and oil concentration distribution at the inlet pressure of 20 MPa and reaction conversion rate at different inlet pressure (with fracture). (**a**) Temperature distribution; (**b**) distributions of oil concentration; (**c**) reaction conversion rate at different inlet pressure.

3.3. Performance Comparison for In Situ Pyrolysis of Oil-Rich Coal with Various Areas of the Fractured Zone

The results in the above section indicate that the heat and mass transfer can be effectively enhanced during pyrolysis by increasing the permeability. However, the cost for fracturing will also increase distinctly for a larger area of fracturing execution whether using hydrofracturing or shock wave fracturing. Thus, it is essential to determine the appropriate diameter near the inlet and the outlet well. In this section, three different areas of fractured zone are investigated to find out their effect on the performance of pyrolysis of the oil-rich coal underground. The diameter of the fractured zone is set as 4 m, 5 m and 6 m, respectively, as shown in Figure 2. The injection gauge pressure is set as 1 MPa. For the fractured zone with high permeability, ϑ is set to 1000 md, and for the unfractured zone, ϑ is set to 100 md. The temperature distributions of these three cases on the 30th, 90th and 180th day are shown in Figure 8a–c. And the reaction conversion rate comparison is shown in Figure 8d. It is seen that with the increase in the fractured zone area or diameter, the high-temperature region increases within the same reaction time, as shown in Figure 8a–c. Thus, the conversion rate is higher with a larger diameter of the fractured zone, as shown in Figure 8d. And the dead zones around the two corners at the right side of the computational domain near the outlet well are also reduced effectively on the 180th day. However, the dead zones are still obvious before the 180th day for the reason that the fractured region near the outlet has less effect on the evolution of the temperature field at the preceding stage of pyrolysis. On the other hand, the overlapping fractured region does not contribute much to the overall pyrolysis performance of the coal. Thus, in the following section, a different radius of the fractured region at the inlet and outlet without overlapping is employed, and the pyrolysis performance is investigated and compared.

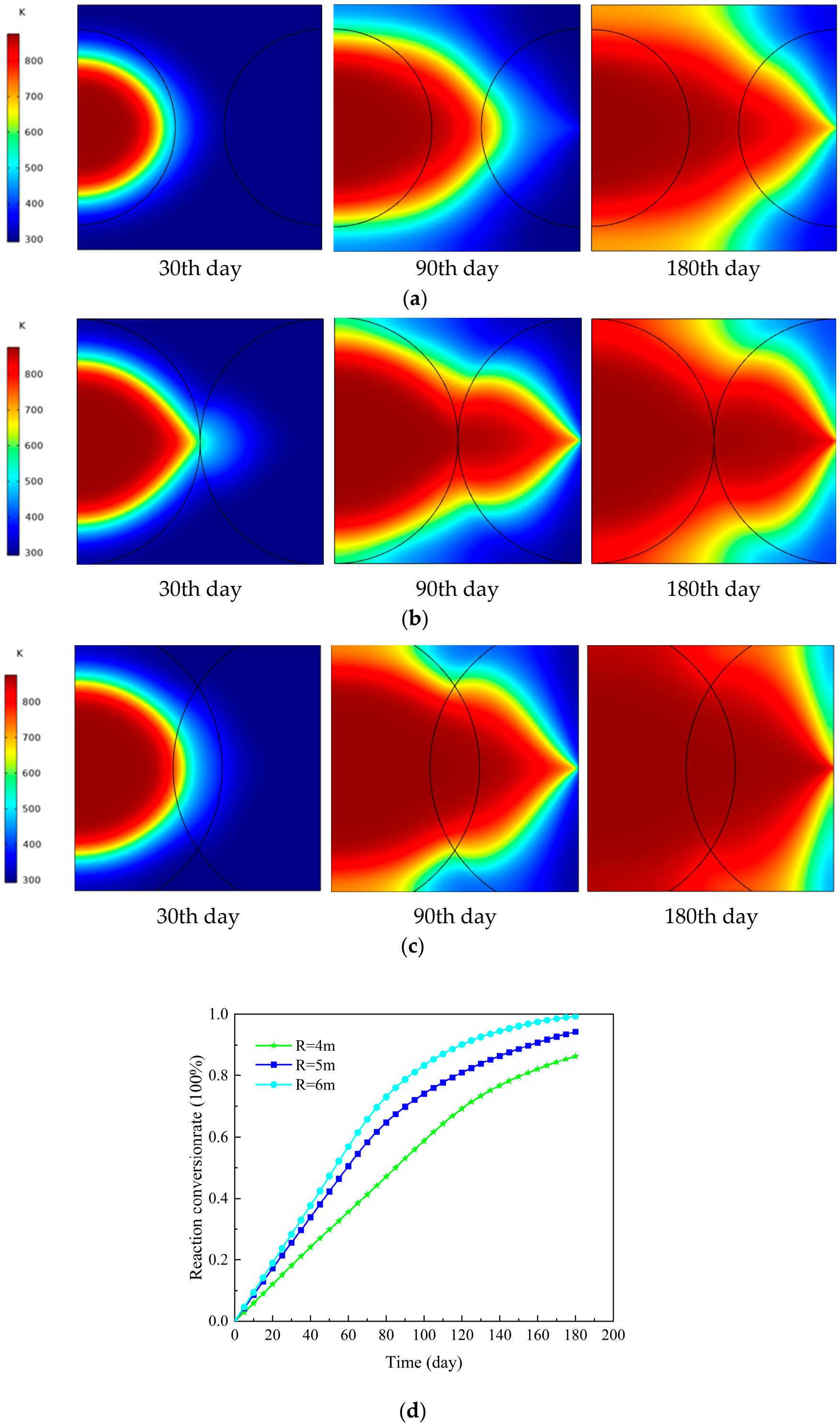

Figure 8. Temperature distribution and reaction conversion rate with different radius of fractured zone. (**a**) R = 4 m; (**b**) R = 5 m; (**c**) R = 6 m; (**d**) reaction conversion rate with different radius of fractured zone.

3.4. Effect of the Area of the Fractured Zone at the Outlet Well

In this section, seven different combinations of the fractured region radius of the inlet and outlet zone are investigated. The results are shown in Figure 9a. R1 indicates the radius of the fractured zone in the area where the inlet is located. R2 indicates the radius of the fractured zone in the area where the outlet is located. It is shown that the initial conversion rate is almost the same with different radius of the inlet and outlet fractured region, since the effective gas diffusion area is similar. However, for the case with a larger radius of the fractured region near the outlet, the subsequent conversion rate is higher. Thus, the total pyrolysis time is shorter. The reason is that the larger fractured region near the outlet well offers a larger hot fluid diffusion area with a lower flow resistance, and the flowing 'dead zone' could also experience a longer effective heating time, as shown in Figure 9b,c. Thus, the heat and mass transfer are enhanced and pyrolysis is promoted.

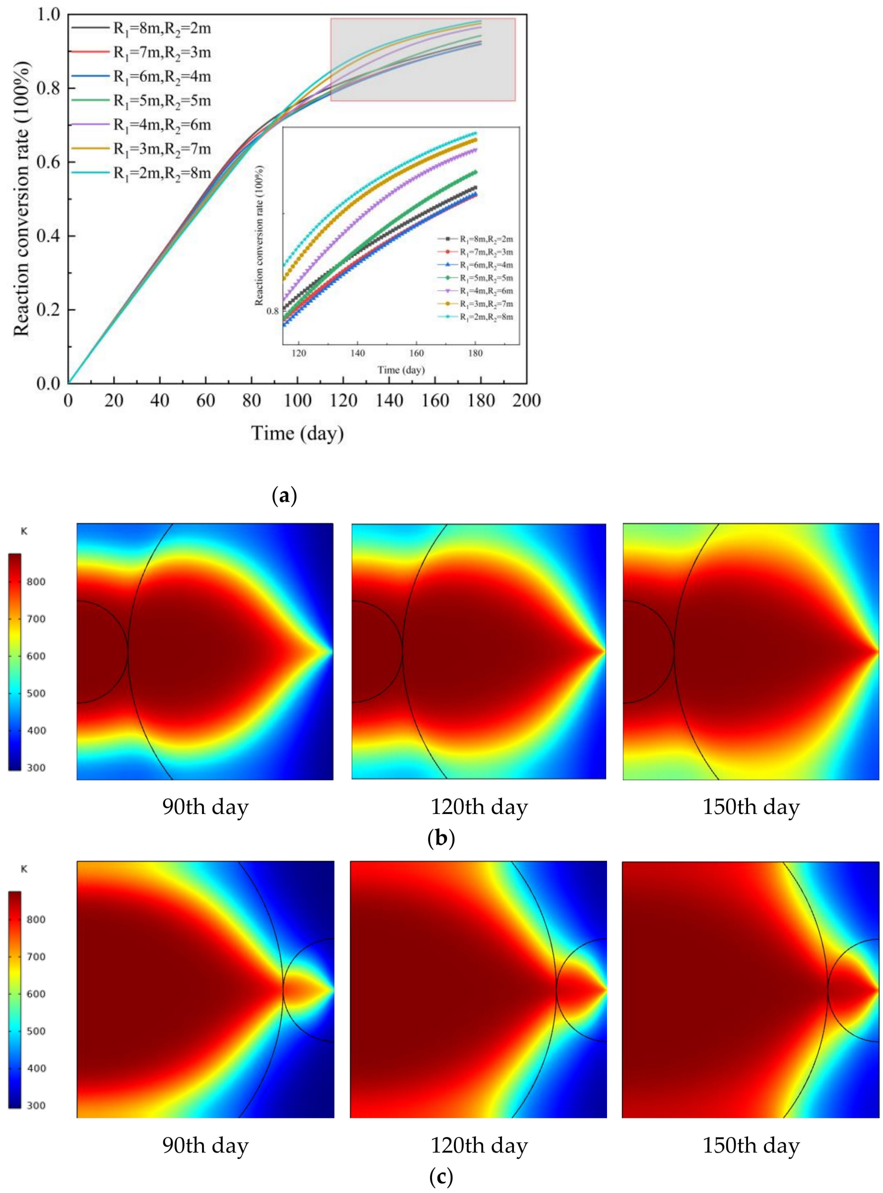

Figure 9. Reaction conversion rate and temperature distribution with different areas of the fractured zone at the outlet well. (**a**) Reaction conversion rate with different area of the fractured zone; (**b**) R_1 = 2 m, R_2 = 8 m; (**c**) R_1 = 8 m, R_2 = 2 m.

4. Conclusions

In this paper, the numerical prediction model of in situ pyrolysis of oil-rich coal in engineering application was obtained. The engineering performance of in situ pyrolysis is predicted, and heat and mass transfer are enhanced by fracturing the coal reservoir at various areas near the inlet and the outlet wells, which provides technical support and theoretical guidance for the pilot project of in situ pyrolysis of oil-rich coal underground. The conclusions can be obtained as follows:

(1) For the model without fracture, the conversion rate on the 120th day is 98.8% when the injection gauge pressure is increased to 14 MPa, and the promotion is not obvious any more with further higher pressure.
(2) For the model with fracture, pyrolysis can be completed in only 90 days at a much lower pressure of 4 MPa, which is beneficial for both reducing the heating period and the rapid harvesting of oil production.
(3) The dead zones around the two corners at the right side of the computational domain near the outlet well are reduced effectively when the diameter of the fractured zone is increased.
(4) The heat and mass transfer can be enhanced with the larger area of the fractured region at the outlet well for the reason that the flowing 'dead zone' experienced a longer effective heating time.

Author Contributions: Conceptualization, M.L. and F.Y.; methodology, M.L.; software, M.L. and X.C.; validation, F.Y., X.C. and M.L.; formal analysis, X.C. and M.L.; investigation, F.Y. and X.C.; resources, F.Y., L.M. and Z.D.; data curation, X.C.; writing—original draft preparation, X.C.; writing—review and editing, X.C. and M.L; visualization, F.Y. and L.M.; supervision, M.L. and J.W.; project administration, F.Y., Z.D. and J.W.; funding acquisition, M.L. and J.W. All authors have read and agreed to the published version of the manuscript.

Funding: This study is supported by the Research Project of Shaanxi Provincial Coal Geology Group Co., Ltd. (No. SMDZ-2020ZD-1-02), the Special Project on Energy Safety Technology of China Huaneng Group Co., Ltd. (HNKJ20-H8), "Scientists + Engineers" team for in situ Hydrogen Production and Comprehensive Utilization of oil-rich coal in Shaanxi Province (2022KXJ-126) and Natural Science Basic Research Program of Shaanxi Province on Pore Evolution and Hydrocarbon migration Mechanism during In situ Pyrolysis of oil-rich coal (2022KJXX-24).

Data Availability Statement: Data is contained within the article.

Conflicts of Interest: The authors declare that this study received funding from Shaanxi Provincial Coal Geology Group Co., Ltd. The funder had the following involvement with the study: collection, analysis, the decision to submit it for publication.

References

1. Wang, S.; Shi, Q.; Wang, S.; Shen, Y.; Sun, Q.; Cai, Y. Resource property and exploitation concepts with green and low-carbon of tar-rich coal as coal-based oil and gas. *J. China Coal Soc.* **2021**, *46*, 1365–1377.
2. Ma, L.; Tuo, B. Shaanxi's tar-rich coal resources rank first in China-Yulin can be "rebuilt a Daqing oilfield". *Shaanxi Coal* **2020**, *39*, 220–222.
3. Pei, S.; Cui, G.; Zhang, L.; Zhang, P.; Ren, S. Performance and important engineering aspects of air injection assisted in situ upgrading process for heavy oil recovery. *J. Pet. Sci. Eng.* **2021**, *202*, 108554.
4. Pei, S.; Wang, Y.; Liang, Z.; Huang, L.; Cui, G.; Zhang, P.; Ren, S. An innovative nitrogen injection assisted in-situ conversion process for oil shale recovery: Mechanism and reservoir simulation study. *J. Pet. Sci. Eng.* **2018**, *171*, 507–515.
5. Zhao, W.; Hu, S.; Hou, L. Connotation and strategic role of in-situ conversion processing of shale oil underground in the onshore China. *Pet. Explor. Dev.* **2018**, *45*, 563–572.
6. Song, X.; Zhang, C.; Shi, Y.; Li, G. Production performance of oil shale in-situ conversion with multilateral wells. *Energy* **2019**, *189*, 116145.
7. Mukhina, E.; Cheremisin, A.; Khakimova, L.; Garipova, A.; Dvoretskaya, E.; Zvada, M.; Kalacheva, D.; Prochukhan, K.; Kasyanenko, A.; Cheremisin, A. Enhanced oil recovery method selection for shale oil based on numerical simulations. *ACS Omega* **2021**, *6*, 23731–23741.
8. Maes, J.; Muggeridge, A.H.; Jackson, M.; Quintard, M.; Lapene, A. Scaling analysis of the in-situ upgrading of heavy oil and oil shale. *Fuel* **2017**, *195*, 299–313.

9. Lee, K.J.; Moridis, G.J.; Ehlig-Economides, C.A. Numerical simulation of diverse thermal in situ upgrading processes for the hydrocarbon production from kerogen in oil shale reservoirs. *Energy Explor. Exploit.* **2017**, *35*, 315–337.
10. Pei, S.; Cui, G.; Wang, Y.; Zhang, L.; Ren, S. Air assisted in situ upgrading via underground heating for ultra heavy oil: Experimental and numerical simulation study. *Fuel* **2020**, *279*, 118452.
11. Wang, L.; Yang, D.; Kang, Z. Evolution of permeability and mesostructure of oil shale exposed to high-temperature water vapor. *Fuel* **2021**, *290*, 119786.
12. Lee, K.J.; Moridis, G.J.; Ehlig-Economides, C.A. In situ upgrading of oil shale by steamfrac in multistage transverse fractured horizontal well system. *Energy Sources Part A Recovery Util. Environ. Eff.* **2016**, *38*, 3034–3041.
13. Gao, W.; Zagorščak, R.; Thomas, H.R. Insights into solid-gas conversion and cavity growth during Underground Coal Gasification (UCG) through Thermo-Hydraulic-Chemical (THC) modelling. *Int. J. Coal Geol.* **2021**, *237*, 103711.
14. Panahi, H.; Kobchenko, M.; Meakin, P.; Dysthe, D.K.; Renard, F. In-situ imaging of fracture development during maturation of an organic-rich shale: Effects of heating rate and confinement. *Mar. Pet. Geol.* **2018**, *95*, 314–327.
15. Jiang, L.; Chen, Z.; Ali, S.M.F. Thermal-hydro-chemical-mechanical alteration of coal pores in underground coal gasification. *Fuel* **2020**, *262*, 116543.
16. Wang, G.; Yang, D.; Kang, Z.; Zhao, J.; Lv, Y. Numerical investigation of the in situ Oil Shale pyrolysis process by superheated steam considering the anisotropy of the thermal, hydraulic, and mechanical characteristics of oil shale. *Energy Fuels* **2019**, *33*, 12236–12250.
17. Yuan, J.; Jiang, R.; Cui, Y.; Xu, J.; Wang, Q.; Zhang, W. The numerical simulation of thermal recovery considering rock deformation in shale gas reservoir. *Int. J. Heat Mass Transf.* **2019**, *138*, 719–728.
18. Hu, L.; Li, H.; Babadagli, T.; Xie, X.; Deng, H. Thermal stimulation of shale formations by electromagnetic heating: A clean technique for enhancing oil and gas recovery. *J. Clean. Prod.* **2020**, *277*, 123197.
19. Alfarge, D.; Wei, M.; Bai, B. Factors affecting CO_2-EOR in shale-oil reservoirs: Numerical simulation study and pilot tests. *Energy Fuels* **2017**, *31*, 8462–8480.
20. Gür, M.; Canbaz, E.D. Analysis of syngas production and reaction zones in hydrogen oriented underground coal gasification. *Fuel* **2020**, *269*, 117331.
21. Xi, J.; Liang, J.; Sheng, X.; Shi, L.; Li, S. Characteristics of lump lignite pyrolysis and the influence of temperature on lignite swelling in underground coal gasification. *J. Anal. Appl. Pyrolysis* **2016**, *117*, 228–235.
22. Zhou, Y.; Li, L.; Jin, L.; Zhu, J.; Li, J.; Li, Y.; Fan, H.; Hu, H. Effect of functional groups on volatile evolution in coal pyrolysis process with in-situ pyrolysis photoionization time-of-flight mass spectrometry. *Fuel* **2020**, *260*, 116322.
23. Xiong, Y.; Jin, L.; Li, Y.; Zhou, Y.; Hu, H. Structural features and pyrolysis behaviors of extracts from microwave-assisted extraction of a low-rank coal with different solvents. *Energy Fuels* **2019**, *33*, 106–114.
24. Shu, P.; Yu, L.; Ming, D. Pyrolysis characteristics and kinetics of the marine microalgae *Dunaliella tertiolecta* using thermogravimetric analyzer. *Bioresour. Technol.* **2010**, *101*, 359–365.
25. Boonchom, B.; Puttawong, S. Thermodynamics and kinetics of the dehydration reaction of $FePO_4{\cdot}2H_2O$. *Phys. B Condens. Matter.* **2010**, *405*, 2350–2355.
26. Yorulmaz, S.; Atimtay, A. Investigation of combusition kinetics of treated and untreated waste wood samples with thermogravimetric analysis. *Fuel Process. Technol.* **2009**, *90*, 939–946.
27. Fu, X.; Zhong, Z.; Xiao, G.; Li, R. Comparative study on characteristics and dynamics of pyrolysis process of grass biomass. *Boil. Technol.* **2011**, *42*, 60–64.